

# Buckling of Sandwich Panels under Nonuniform Stress

R. A. GELLATLY,\* P. P. BIJLAARD,† AND R. H. GALLAGHER‡  
*Textron's Bell Aerosystems Company, Buffalo, N. Y.*

A procedure is developed for the determination of the critical buckling stress of long sandwich panels subjected to nonuniformly distributed longitudinal loads at the ends. The procedure is based on a reduction of the governing partial differential equation by introduction of the longitudinal deflection shape and solution of the resulting ordinary differential equation by means of second-order finite differences. Design charts are developed for linear and trigonometric-shaped stress distributions for a range of stiffnesses that extends to the isotropic thin plate at one limit. Illustrative examples, including comparisons with pertinent isotropic plate solutions, are presented.

## Nomenclature

$b$	= panel width, in.
$D_q$	= sandwich shear stiffness, lb/in.
$D_s$	= sandwich bending stiffness, in.-lb
$D$	= sandwich panel stiffness parameter
$h$	= depth of sandwich core, in.
$k$	= buckling coefficient
$S$	= stress ratio
$t$	= face thickness of sandwich panel, in.
$w$	= transverse displacement
$W$	= displacement function
$\lambda, \Lambda$	= wavelength parameters
$\mu$	= Poisson's ratio
$\Pi$	= critical stress parameter
$\rho$	= stress-distribution parameter
$\sigma$	= stress, psi

## I. Introduction

SANDWICH panels provide an attractive constructional form for the skins of large high-performance vehicles. They are extremely efficient from a weight standpoint and can be fabricated using materials suitable for an elevated temperature environment exceeding 1000°F. Sufficient data have been accumulated to permit their design for conventional loadings and uniform temperature conditions (c.f., Ref. 1), but design data are lacking for nonuniform temperature conditions. One of the most important problems in this latter category is the prediction of elastic instability in the presence of nonuniform stresses produced by temperature gradients. The lack of design information for this problem extends, in fact, to the simpler case of isotropic thin plates. Hoff,<sup>2</sup> Klosner and Forray,<sup>3</sup> Van Der Neut,<sup>4</sup> and Kollbrunner and Meister,<sup>5</sup> among others, have developed methods of solution for the problem of isotropic plate stability under nonuniform stress. No design curves are available, however, for cases such as the cosine-shaped stress distribution, which represents an approximation to an important multiweb wing-thermal stress problem. The authors are unaware of published solution procedures for sandwich panels.

The present paper develops a finite-difference solution procedure for the instability analysis of honeycomb sandwich

panels with equal thickness isotropic skins under nonuniform longitudinal stress. The panels are assumed to be "long" (i.e., aspect-ratio effects and the significance of the transverse support conditions are excluded) and simply supported along their longitudinal edges. The conditions of analysis are illustrated in Fig. 1. Extensive computations have been performed with the subject procedure, and the results are presented herein in the form of design charts. The charts cover a wide range of stress-distribution parameters for linear and trigonometric-shaped stress distributions, and stiffness parameters that extend from deep sandwich panels with thin faces to isotropic plates. Values obtained from the design charts are then checked against the isolated known solutions.

## II. Theoretical Basis

The classical governing differential equation, for the stability of an isotropic plate of thickness  $t'$  subjected to uniaxial compressive stress  $\sigma_x$ , is

$$D_s \nabla^4 w + t' \sigma_x (\partial^2 w / \partial x^2) = 0 \quad (1)$$

Equation (1) can be transformed into an equation applicable to the case of a sandwich plate, composed of equal thickness isotropic faces possessing only stiffness in direct stress and an isotropic core, which possesses only shear stiffness, by modifying it to include the effect of the shear deformability of the core.<sup>6</sup> With this modification, Eq. (1) becomes

$$D_s \nabla^4 w + [1 - (D_s/D_q) \nabla^2] 2t \sigma_x (\partial^2 w / \partial x^2) = 0 \quad (1a)$$

where  $D_s$  is the bending stiffness and  $D_q$  is the core shear stiffness. The analyst has at his disposal the choice of a number of formulas for  $D_s$  and  $D_q$ , dependent upon the details of sandwich panel construction; these choices are developed and discussed in Ref. 1, Sec. 3.1.

To solve Eq. (1a) the displacement  $w$  is first assumed as

$$w = W \sin \lambda x \quad (2)$$

where  $W$  is a function of  $y$  only, and  $\lambda$  is a parameter involving the buckle wavelength in the longitudinal ( $x$ ) direction. Using Eq. (2) in Eq. (1a) and introducing a nondimensionalization of the stress distribution through use of  $\rho = \sigma_x / \sigma_{cr}$ , one obtains

$$[\lambda^4 W - 2 \lambda^2 W'' + W^{iv}] - \frac{2t \sigma_{cr} \lambda^2}{D_s} \left[ \left( 1 + \frac{D_s \lambda^2}{D_q} \right) \times \right. \\ \left. \rho W - \frac{D_s}{D_q} (\rho W)'' \right] = 0 \quad (3)$$

where the primes on  $W$  indicate derivatives with respect to  $y$ . Note that the introduction of  $\rho$  serves to establish a single parameter ( $\sigma_{cr}$ ) that characterizes instability in the presence of nonuniformly distributed stresses.

Received December 10, 1963; revision received January 15, 1965. Work described herein was performed in conjunction with a Federal Aviation Agency sponsored study, Contract No. AF33(657)-8936, "Thermal Stress Determination Techniques for Supersonic Transport Aircraft Structures." The authors are deeply appreciative to Leona Barback for her efforts in the computer programming phases of this effort.

\*Structures Research Engineer, Aerospace Engineering Department.

†Consultant; also Professor of Engineering Mechanics, Cornell University, Ithaca, N. Y. Member AIAA.

‡Chief, Advanced Airframe Analysis. Associate Fellow Member AIAA.

Table 1 [A] matrix

	$W_1$	$W_2$	$W_3$	$W_4$	$W_5$	$W_6$	$W_7$	$W_8$
1	$112 + 60 \left(\frac{\Lambda}{81}\right) + 12 \left(\frac{\Lambda}{81}\right) - \left[24 + 2 \left(\frac{\Lambda}{81}\right)\right]$							
2	$-78 - 32 \left(\frac{\Lambda}{81}\right) + 2$	$112 + 60 \left(\frac{\Lambda}{81}\right) + 12 \left(\frac{\Lambda}{81}\right)^2$						
3	$24 + 2 \left(\frac{\Lambda}{81}\right)$	$-78 - 32 \left(\frac{\Lambda}{81}\right)$	$112 + 60 \left(\frac{\Lambda}{81}\right) + 12 \left(\frac{\Lambda}{81}\right)^2$					
4	-2	$24 + 2 \left(\frac{\Lambda}{81}\right)$	$-78 - 32 \left(\frac{\Lambda}{81}\right)$	$112 + 60 \left(\frac{\Lambda}{81}\right) + 12 \left(\frac{\Lambda}{81}\right)^2$				
5	0	-2	$24 + 2 \left(\frac{\Lambda}{81}\right)$	$-78 - 32 \left(\frac{\Lambda}{81}\right)$	$112 + 60 \left(\frac{\Lambda}{81}\right) + 12 \left(\frac{\Lambda}{81}\right)^2$			
6	0	0	-2	$24 + 2 \left(\frac{\Lambda}{81}\right)$	$-78 - 32 \left(\frac{\Lambda}{81}\right)$	$112 + 60 \left(\frac{\Lambda}{81}\right) + 12 \left(\frac{\Lambda}{81}\right)^2$		
7	0	0	0	-2	$24 + 2 \left(\frac{\Lambda}{81}\right)$	$-78 - 32 \left(\frac{\Lambda}{81}\right)$	$112 + 60 \left(\frac{\Lambda}{81}\right) + 12 \left(\frac{\Lambda}{81}\right)^2$	
8	0	0	0	0	-2	$24 + 2 \left(\frac{\Lambda}{81}\right)$	$-78 - 32 \left(\frac{\Lambda}{81}\right) + 2$	$112 + 60 \left(\frac{\Lambda}{81}\right) + 12 \left(\frac{\Lambda}{81}\right)^2 - \left[24 + 2 \left(\frac{\Lambda}{81}\right)\right]$

(Symmetric)

Finite differences are used to reduce this equation to algebraic form. With nine intervals (Fig. 1) and second-order finite differences,<sup>7</sup> one obtains the following evaluation of Eq. (3) at an arbitrary interior point  $k$ :

$$\{-2[W_{k-3} + W_{k+3}] + [W_{k-2} + W_{k+2}][24 + \frac{2}{3}\Lambda] - [W_{k-1} + W_{k+1}][78 + \frac{3}{2}\Lambda] + W_k \times [112 + \frac{2}{9}\Lambda + 12(\Lambda/81)^2]\} - \Pi\Lambda/81\{\rho_{k-2}W_{k-2} - 16\rho_{k-1}W_{k-1} + [30 + \frac{4}{9}\Lambda + \frac{4}{9}D]\rho_k W_k - 16\rho_{k+1}W_{k+1} + \rho_{k+2}W_{k+2}\} = 0 \quad (4)$$

where

$$\Pi = 2t\sigma_{cr}/D_q \quad D = D_q b^2/D_s \quad \Lambda = (\lambda b)^2$$

The boundary conditions for  $W$  are

$$W_0 = W_9 = 0 \quad W_{-1} = -W_1 \quad W_{-2} = -W_2 \\ W_{10} = -W_8 \quad W_{11} = -W_7$$

The boundary conditions on  $\rho$  must be based on an extrapolation of the stress distribution beyond the edges of the plate. (Although there is no loading outside of the edges of the plate, i.e., in actuality  $\rho_i = 0$  for  $i < 0$  and  $i > 9$ , the use of finite differences requires the introduction of fictitious exterior loadings, if the stress variation in the intervals adjacent to the edges are to be represented properly.)

With use of the boundary conditions, Eq. (4) can be adapted to each of the eight internal points, obtaining thereby eight simultaneous equations with coefficients  $W_1, \dots, W_8$ .

These equations can be written in matrix form as follows

$$([A] - \Pi\Lambda[B])\{W\} = 0 \quad (5)$$

The matrices  $[A]$  and  $[B]$  are presented in Tables 1 and 2, respectively.

The condition for buckling is that the determinant of Eq. (5) shall vanish. A more attractive solution procedure is through matrix iteration, however, since direct evaluation of the determinant would lead to a somewhat complex polynomial of eighth order in  $\Pi$ . To permit matrix iteration, Eq. (5) is rearranged as follows:

$$1/\Pi\Lambda\{W\} = [A]^{-1}[B]\{W\} \quad (6)$$

Then, iteration of Eq. (6) is performed, starting with an initially assumed vector  $\{W\}$ , until convergence on the eigenvector  $\{W\}_{cr}$  and eigenvalue  $(1/\Pi\Lambda)_{cr}$  is achieved.

For this type of problem it has been found, under certain conditions, that an oscillation will occur in the iterative process. The process converges on two different vectors, such that the vectors  $\{W\}_p, \{W\}_{p+2}$  are identical, and  $\{W\}_{p+1}, \{W\}_{p+3}$  are identical (the subscript  $p$  designates the  $p$ th iterative cycle). This case occurs when the matrix being iterated upon has two roots equal in magnitude, but differing in sign. The relevant eigenvalues are then the two square roots of the product of the two apparent eigenvalues, i.e.,

$$(1/\Pi\Lambda)_{cr} = \pm [(1/\Pi\Lambda)_p(1/\Pi\Lambda)_{p+1}]^{1/2} \quad (7)$$

Table 2 [B] matrix<sup>a</sup>

	$W_1$	$W_2$	$W_3$	$W_4$	$W_5$	$W_6$	$W_7$	$W_8$
1	$+L\rho_1 - \rho_{-1}$	$-16\rho_2$	$+\rho_3$	0	0	0	0	0
2	$-16\rho_1$	$+L\rho_3$	$-16\rho_3$	$+\rho_4$	0	0	0	0
3	$+\rho_1$	$-16\rho_2$	$+L\rho_3$	$-16\rho_4$	$+\rho_5$	0	0	0
4	0	$+\rho_2$	$-16\rho_3$	$+L\rho_4$	$-16\rho_5$	$+\rho_6$	0	0
5	0	0	$+\rho_3$	$-16\rho_4$	$+L\rho_5$	$-16\rho_6$	$+\rho_7$	0
6	0	0	0	$+\rho_4$	$-16\rho_5$	$+L\rho_6$	$-16\rho_7$	$+\rho_8$
7	0	0	0	0	$+\rho_5$	$-16\rho_6$	$+L\rho_7$	$-16\rho_8$
8	0	0	0	0	0	$+\rho_6$	$-16\rho_7$	$+L\rho_8 - \rho_{10}$

<sup>a</sup> Where  $L = [(12D_p/81) + (12\Lambda/81) + 30]$ .

The previous condition occurs in practice when the applied loading is a bending moment across the width of the panel. (It is obvious that the same value of moment will induce buckling independent of whether the moment acts in either of two opposing directions.) The analysis procedure, as described previously, yields a critical stress that corresponds to one preselected value of  $\lambda$ , the buckling wavelength parameter. As  $\lambda$  is varied, the critical stress will vary, reaching a minimum for an as-yet unknown value of  $\lambda$ . To establish this absolute minimum, one can first select a range of  $\lambda$ 's and calculate for each the corresponding critical-stress parameter,  $\Pi$ . Next, employing these results, a polynomial  $\Pi$  vs  $\lambda$  relationship is established through use of a curve-fitting technique. The minimum  $\Pi$  is then obtained through solution of the equation resulting from the condition  $d\Pi/d\lambda = 0$ .

### III. Design Charts

The foregoing procedure was applied to the development of design data for a wide range of stiffnesses and load conditions. An IBM 7090 computer program, coded for the purpose of obtaining the critical stress for any given stress distribution, was utilized to generate this data. In order to establish effectively convergent results, all computations were performed for two mesh sizes, the first being the 9-interval solution detailed in this paper and the second an 18-interval scheme. In general, the differences between the results for the two schemes were of the order of 0.4%. In view of the unavoidable inaccuracies in the graphical representations that have been made of the computed results, the usefulness of any improvement of the results through an extrapolation technique is negated.

The value of the critical buckling stress parameter is a function of 1) the buckle wavelength (represented by the parameter  $\lambda$ ), 2) the panel stiffness (represented by the parameter  $D$ ), and 3) the applied-load distribution (described by the parameter  $\rho$ ). Wavelength considerations are taken into account by the scheme described previously. Thus, it is only necessary to decide which ranges of the parameters  $D$  and  $\rho$  are of practical interest.

In the strictest sense, the stiffness parameter  $D$  can range from nearly zero to infinity. At infinity the case of the isotropic plate with infinite shear stiffness prevails. This

condition is nearly achieved at much lower values, and it is satisfactory to consider the maximum  $D$  to equal  $10^4$ . At the lower range of  $D$ , it is found that an entirely different mode of instability, wrinkling, is encountered. This mode is characterized by a zero-wavelength buckling condition due to an initial assumption that the individual bending stiffnesses of the faces could be neglected. Since it is not the intention of the present analysis to deal with wrinkling, the curves have been terminated at  $N_x/(h + t)G_c = 1$ , which is a limit imposed by wrinkling associated with shear instability failure of the core. Thus, evaluations of the critical stress were performed for a range of  $D$  values from  $10^4$  down to values where this shear instability limit appeared.

Only the simplest forms of stress distribution are of general interest and therefore suitable for inclusion in design charts. The results presented herein were developed for linear and trigonometric-shaped stress distributions. Linear or nearly linear distributions exist on panels in wings sustaining over-all nonuniform chordwise temperature gradients and also when the bending stress distribution on a stiffened skin departs from the uniformity predicted by elementary theory (as is generally the case). Trigonometric-shaped stress distributions are good approximations of conditions where the panel longitudinal edge members (e.g., spar caps) provide significant heat sinks, thereby resulting in extreme, local, transverse variations of the longitudinal thermal stress.

A linear variation of stress, which is equivalent to a uniformly distributed load superimposed upon a bending moment, is conveniently described by the ratio ( $S$ ) of the stress levels at either side of the panel. Using the convention that the denominator is always the larger positive (compressive) value, any purely compressive load is covered by the range  $1 \geq S \geq 0$ . This range has been extended into the mixed compressive-tensile region to the value  $S = -1.0$ , i.e., pure bending. This range of  $S$  from  $+1.0$  to  $-1.0$  has been covered in intervals of 0.25. The selected trigonometric cases are simply  $\sin \pi y/b$ ,  $\sin 2\pi y/b$ ,  $\cos \pi y/b$ ,  $\cos 2\pi y/b$ .

Figures 1 and 2 present the results in graphical form. It was intended to depict in Fig. 1 the results from Ref. 1 for uniform compression ( $S = 1.0$ ), but because of the excellent level of agreement, it is not possible to differentiate between those results and the present solutions for  $S = 1.0$ . The

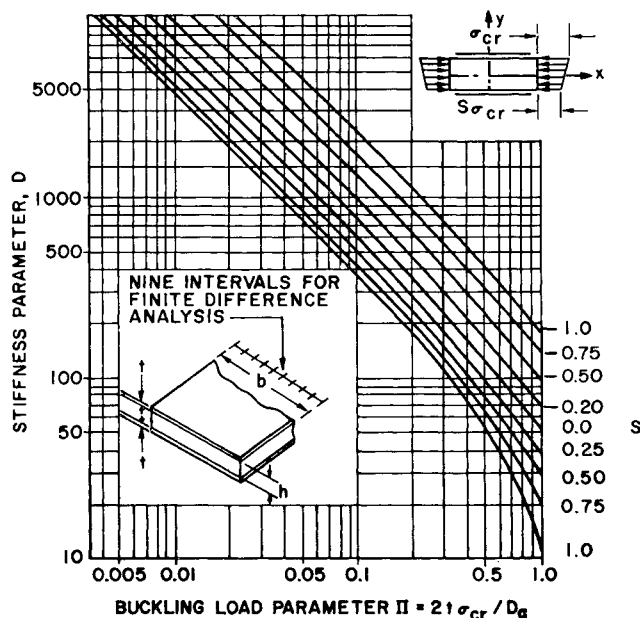


Fig. 1 Buckling parameter for linearly varying edge stress; long edges simply supported.

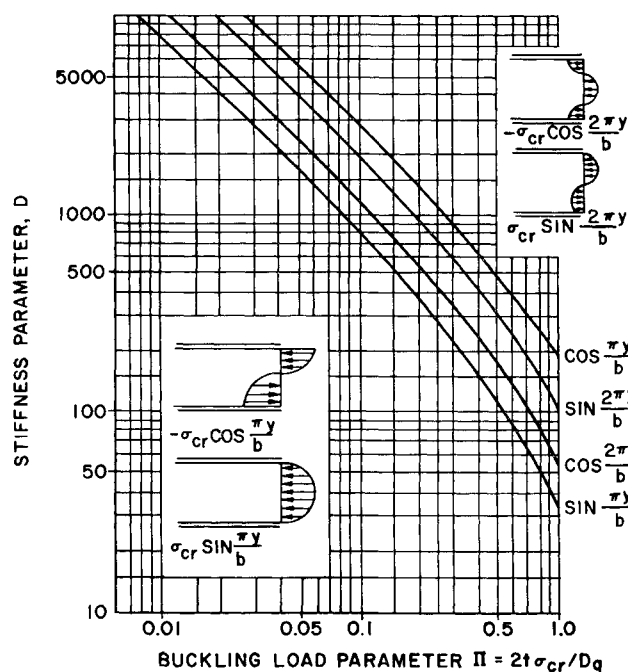


Fig. 2 Buckling parameters for trigonometric-shaped edge stresses; long edges simply supported.

**Table 3 Comparison of results**

$S$	$h$	
	Timoshenko	Present results
+1.0	4.00	3.98
0	7.81	7.79
-0.5	13.40	13.35
-1.0	23.90	23.63

curves are terminated at the lower end by the wrinkling boundary discussed previously.

Figure 3 depicts the variation of buckling stress for the isotropic plate subject to linear stress distributions. These curves have been obtained by considering large values of  $D$ . Here, the form of the ordinate has been altered to eliminate the shear stiffness of the core ( $D_q$ ). The new ordinate is thus taken as  $\sigma_{cr} t_i b^2 / DS$  where  $t_i = 2t$  is the thickness of the isotropic plate.

Illustrative examples are as follows:

1) A sandwich plate with simply supported edges has a width of panel of 40 in., a core thickness of 0.50 in., a modulus of faces of  $10^7$  psi, a face thickness of 0.036 in., and a shear modulus of core of  $2 \times 10^4$  psi. The panel is subjected to a triangular compressive load ( $S = 0$ ). Utilizing the preceding data and formulas (3.12E) and (3.13B) from Ref. 1, one obtains  $D_s = 5.68 \times 10^4$ ,  $D_q = 1.0 \times 10^4$ , and  $D = D_q b^2 / D_s = 282$ . From Fig. 1, for  $S = 0$  at  $D = 282$ , the buckling-load parameter  $2t\sigma_{cr}/D_q$  is found to be 0.257. Hence,

$$\sigma_{cr} = 0.257 D_q / 2t = 35,700 \text{ psi}$$

The total applied load =  $t \sigma_{cr} b = 51,400$  lb.

2) An isotropic plate with simply supported edges has a width of panel of 40 in., a modulus of panel of  $10^7$  psi, and a thickness of 0.388 in.; thus  $D_s = 5.343 \times 10^4$ .

This panel is also subjected to a triangular compression ( $S = 0$ ). From Fig. 3 at  $S = 0$ ,  $t_i b^2 \sigma_{cr} / D_s = 77.05$ . Thus,

$$\sigma_{cr} = 77.05 D_s / t_i b^2 = 6625 \text{ psi}$$

Here again total applied load ( $= t_i \sigma_{cr} b / 2$ ) = 51,400 lb. Thus, the two panels carry the same loading but, as can be seen, the sandwich panel has a considerable advantage over the isotropic plate on a weight basis.

The published solutions for buckling of long panels under nonuniform loading are entirely restricted to the case of isotropic plates. Timoshenko<sup>8</sup> has considered an isotropic plate with a linearly varying stress. The parameter used by Timoshenko is the factor  $k$  in the expression

$$\sigma_{cr} = k \pi^2 D_s / t b^2$$

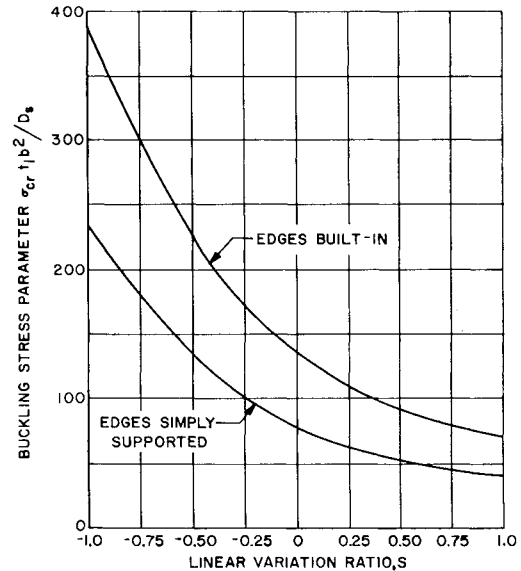


**Fig. 3 Buckling parameters for isotropic plates subject to linearly varying compressive loading.**

Using this parameter, a comparison is obtained from Table 3. Hoff<sup>2</sup> has considered a trigonometric distribution of load, corresponding to the  $\cos 2\pi y/b$  case of the present paper. The value obtained by Hoff ( $k = 7.67$ ) shows good agreement with the present work where  $k = 7.68$ .

## References

- <sup>1</sup> "Sandwich construction for aircraft," Air Force, Navy, Commerce Bull. ANC 23, Part II (1955).
- <sup>2</sup> Hoff, N. J., "Thermal buckling of supersonic wing panels," J. Aeronaut. Sci. **23**, 1019-1028 (1956).
- <sup>3</sup> Klosner, J. and Forray, M., "Buckling of simply supported plates under arbitrary symmetrical temperature distributions," J. Aeronaut. Sci. **25**, 181-184 (1958).
- <sup>4</sup> VanDerNeut, A., "Buckling caused by thermal stresses," *High Temperature Effects in Aircraft Structures* (Pergamon Press, New York, 1958), Chap. 11, pp. 215-247.
- <sup>5</sup> Kollbrunner, C. F. and Meister, M., *Ausbeulen* (Springer-Verlag, Berlin, 1958).
- <sup>6</sup> Reissner, E., "Finite deflections of sandwich plates," J. Aeronaut. Sci. **15**, 435-440 (1948).
- <sup>7</sup> Bijlaard, P. and Gallagher, R., "Elastic instability of a cylindrical shell under arbitrary circumferential variation of axial stress," J. Aerospace Sci. **27**, 854-859 (1960).
- <sup>8</sup> Timoshenko, S., *Theory of Elastic Stability* (McGraw-Hill Book Co., Inc., New York, 1936), p. 350.